ISSN 2616-5775 Vol. 9, Issue 1: 94-102, DOI: 10.25236/AJCIS.2026.090112

Forecasting BDS Satellite Clock Bias Using Optimized Grey Model Based on Initial Conditions

Quancheng Wang, Ye Yu*, Guodong Jin, Jianwei Zhao, Xiaoyu Gao, Minli Yao

Rocket Force University of Engineering, Xi'an, 710025, Shaanxi, China
**Corresponding author: yuye115@mails.ucas.edu.cn*

Abstract: *A grey model reformulated through initial-condition optimization is presented to advance the predictive performance of satellite clock bias. First, a grey forecasting model is established. Subsequently, initial conditions are determined using the latest components of the raw sequence. The study concludes with an experimental campaign in which the refined grey model, tuned at the initial condition, forecasts BeiDou satellite clock bias, leveraging Wuhan University's precision clock products as ground truth. Comparative experiments confirm that optimizing the initial condition enables the grey model to outperform the classical grey and polynomial approaches in satellite clock bias forecasting. Its 6 h average forecast accuracy and stability reached 0.47ns, representing improvements of 37.56% and 47.50% compared to the grey model's average accuracy and stability, respectively.*

Keywords: *Beidou satellite navigation system; satellite clock bias; initial condition optimization; grey model; accuracy analysis*

1. Introduction

The performance envelope of the Global Navigation Satellite System (GNSS) Positioning, Navigation and Timing (PNT) services is intrinsically linked to the quality of satellite clock bias (SCB) information, because the system is essentially time-referenced [1-2]. Consequently, the precise modelling and forecasting of SCB have become critical factors in enhancing system performance [3]. During the application of GNSS for precise point positioning, establishing SCB forecast models with higher accuracy and stability is essential to enhance positioning precision. Therefore, to secure centimeter-level positioning accuracy in PPP solutions, high-precision forecasting of SCB is a prerequisite.

Recent advances in BeiDou's space and ground segments have correspondingly heightened the demand for higher-accuracy SCB forecasting. To address this, researchers have proposed a series of SCB forecast models. Among these, grey model (GM (1,1)) has gained widespread application in clock bias forecasting for the GNSS due to their straightforward expressions and minimal data requirements for forecasting [4-5]. However, GM (1,1) exhibits certain limitations and conditions for applicability across different scenarios. Over time, outdated information can introduce perturbations into the system, diminishing forecast accuracy [6]. Furthermore, their adaptability across different satellite clocks is limited, and they rely heavily on data accuracy, potentially yielding significant errors [7-8].

To enhance the forecasting accuracy of SCB and address the limitations of traditional GM (1,1), this paper proposes a SCB forecasting method based on an initial condition-optimized GM (1,1). In the first step, the method resorts to a standard technique for fixing the initial condition, thereby ascertaining the newest element of the first-order cumulative series. Subsequently, based on the form of this latest component, the corresponding expression for the grey forecast model is derived. Finally, the estimated initial conditions are calculated and substituted into the GM (1,1) expression to obtain the grey forecast model equation. Forecasting tests were performed on a randomized cohort of six multi-type BeiDou satellites, employing the precise SCB solutions released by Wuhan University's GNSS Analysis Centre as the reference. Comprehensive experiments confirm that the developed technique achieves demonstrable effectiveness and marked superiority. Establishment of optimized grey model based on initial conditions.

ISSN 2616-5775 Vol. 9, Issue 1: 94-102, DOI: 10.25236/AJCIS.2026.090112

2. Establishment of optimized grey model based on initial conditions

2.1 Grey model

Grey-system literature consistently identifies GM (1,1) as the flagship one-variable, first-order model for practical applications. It constitutes a forecasting model based solely on a single-variable first-order differential equation, suitable for forecasting its own data while requiring minimal data for modelling. Its algorithmic principle is as follows [9-15]:

Consider a sequence of SCB data:

$$x^{(0)} = \left\{ x^{(0)}(1), x^{(0)}(2), \cdots, x^{(0)}(n) \right\} \tag{1}$$

The sequence generated by single accumulation is:

$$x^{(1)} = \left\{ x^{(1)}(1), x^{(1)}(2), x^{(1)}(3), \cdots, x^{(1)}(n) \right\} \tag{2}$$

where:

$$x^{(1)}(k) = \sum_{i=1}^{k} x^{(0)}(i), \quad k = 1, 2, 3, \cdots, n \tag{3}$$

As the GM (1,1) employs exponential growth forecasting, the mathematical expression corresponding to the exponential model is:

$$y = a + ce^{b} \tag{4}$$

Establishing a first-order differential equation with constant coefficients for the sequence $x^{(1)}$:

$$\frac{dx^{(1)}t}{dt} + ax^{(1)}t = b \tag{5}$$

where the parameters a represent the development coefficient, and the parameters u denote the grey action quantity.

Solving differential equation (5) yields the exponential primitive function, establishing the corresponding grey differential equation. Integrating both sides of the differential equation yields:

$$\int_{k-1}^{k} \frac{dx^{(1)}(t)}{dt} dt + \int_{k-1}^{k} ax^{(1)}(t) dt = \int_{k-1}^{k} b dt \tag{6}$$

Analyzing the two definite integrals on the left-hand side of equation (6) yields:

$$\int_{k-1}^{k} \frac{dx^{(1)}(t)}{dt} dt = x^{(1)}(k) - x^{(1)}(k-1) = x^{(0)}(k) \tag{7}$$

Analysis of the first definite integral reveals that it represents the sum of the k th and $k-1$th terms of a linear cumulative sequence. Subtracting these yields the k th term of the original data:

$$x^{(1)}(k) - x^{(1)}(k-1) = x^{(0)}(k) \tag{8}$$

Subsequently, analyzing the second definite integral in equation (6) yields:

$$\int_{k-1}^{k} ax^{(1)}(t) dt \approx a \frac{x^{(1)}(k) + x^{(1)}(k-1)}{2} = az^{(1)}(k) \tag{9}$$

The differential equation in this case (5) may be transformed into:

$$x^{(0)}(k) + az^{(1)}(k) = b \tag{10}$$

ISSN 2616-5775 Vol. 9, Issue 1: 94-102, DOI: 10.25236/AJCIS.2026.090112

Yielding the matrix equation:

$$Y = GA \tag{11}$$

where $u = \begin{bmatrix} 1 & 2 \end{bmatrix}^T$, $Y = \left[x^{(0)}, x^{(0)}(1), x^{(0)}(2), \cdots, x^{(0)}(n) \right]^T$, $A = \begin{bmatrix} a & u \end{bmatrix}^T$.

$$Y = \begin{bmatrix} x^{(0)}(2) \\ x^{(0)}(3) \\ \vdots \\ x^{(0)}(n) \end{bmatrix}, G = \begin{bmatrix} -\frac{\left[x^{(1)}(2) + x^{(1)}(1) \right]}{2} & 1 \\ -\frac{\left[x^{(1)}(3) + x^{(1)}(2) \right]}{2} & 1 \\ \vdots & \vdots \\ -\frac{\left[x^{(1)}(n) + x^{(1)}(n-1) \right]}{2} & 1 \end{bmatrix}, A = \begin{bmatrix} a \\ u \end{bmatrix} \tag{12}$$

The least-squares estimator applied to equation (11) furnishes the following optimal solution:

$$\hat{A} = \begin{bmatrix} \hat{a} & \hat{u} \end{bmatrix} = \left(G^T G \right)^{-1} G^T Y \tag{13}$$

Selecting $x^{(1)}(1) = x^{(0)}(1)$ as initial conditions yields the solution:

$$\hat{x}^{(1)}(k+1) = \left(\hat{x}^{(0)}(1) - \frac{\hat{b}}{\hat{a}} \right) e^{-\hat{a}k} + \frac{\hat{b}}{\hat{a}}, \quad k = 0, 1, \cdots, n-1, \cdots \tag{14}$$

where k denotes the number of original data sequences participating in the forecast. Using the above forecast model, data sequences for any future time point can be forecasted.

2.2 Grey model with optimized initial conditions

The selection of initial conditions plays a crucial role in the predictive accuracy of grey model. Different establishment methods reflect varying considerations regarding the weighting of new and old information, directly altering the model's predictive trajectory.

Traditional GM (1,1) employ three methods for initial condition determination: oldest component solution:

$$\hat{c} = \left(x^{(1)}(k) - \frac{\hat{b}}{\hat{a}} \right) e^{\hat{a}k} \tag{15}$$

Newest component solution:

$$\hat{c} = \left(x^{(1)}(N) - \frac{\hat{b}}{\hat{a}} \right) e^{\hat{a}N} \tag{16}$$

Weighted component solution using both newest and oldest components:

$$\hat{c} = \frac{w x^{(1)}(1) + \left[1 - w x^{(1)}(N) \right] - \frac{\hat{b}}{\hat{a}}}{w e^{-\hat{a}} + (1-w) e^{-\hat{a}N}} \tag{17}$$

where N denotes the order of the latest component, corresponding to the following three forms of grey forecasting models:

ISSN 2616-5775 Vol. 9, Issue 1: 94-102, DOI: 10.25236/AJCIS.2026.090112

$$\begin{gathered}\left(1-e^{\hat{a}}\right)\left(x^{(1)}(1)-\frac{\hat{b}}{\hat{a}}\right)e^{-\hat{a}(n-1)} \\ \left(1-e^{\hat{a}}\right)\left(x^{(1)}(N)-\frac{\hat{b}}{\hat{a}}\right)e^{-\hat{a}(n-N)} \\ \left(1-e^{\hat{a}}\right)\frac{wx^{(1)}(1)+(1-w)x^{(1)}(N)-\frac{\hat{b}}{\hat{a}}}{we^{-\hat{a}n}+(1-w)e^{-\hat{a}N}}e^{-\hat{a}n}\end{gathered} \tag{18}$$

The initial components of the GM (1,1) with optimized initial conditions are determined using the latest component solution method. From expression (16), we obtain:

$$x^{(0)}(n)=\left(1-e^{\hat{a}}\right)ce^{-\hat{a}m} \tag{19}$$

When $n \le N$, $\hat{x}^{(0)}(n) \cong \hat{x}^{(0)}(k)$, then the estimated initial condition can be obtained as:

$$\hat{c}=\frac{\hat{x}^{(0)}(k)e^{\hat{a}k}}{1-e^{\hat{a}}} \tag{20}$$

When $k = N$, the estimated initial condition is obtained as:

$$\hat{c}=\frac{\hat{x}^{(0)}(N)e^{\hat{a}N}}{1-e^{\hat{a}}} \tag{21}$$

Substituting equation (20) into equation (13) yields the grey forecast model with optimized initial conditions:

$$\begin{gathered}\hat{x}^{(0)}(n)=x^{(0)}(N)e^{-\hat{a}(n-N)} \\ N=1,2,\cdots,N+1\end{gathered} \tag{22}$$

When $n \ge N$, the forecast values of the grey model after optimizing the initial conditions can be obtained using Equation (21). The flowchart of this model is shown in Figure 1:

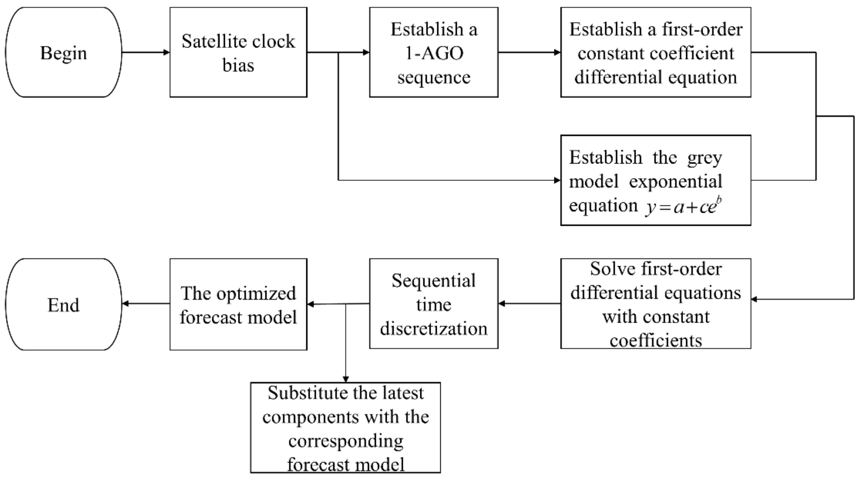

Figure 1: Flowchart of the GM (1,1) model with optimized initial conditions.

ISSN 2616-5775 Vol. 9, Issue 1: 94-102, DOI: 10.25236/AJCIS.2026.090112

3. Experiments and analysis

3.1 Experimental data sources

The experimental validation relies on the precise post-processed clock products of BDS satellites provided by the GNSS Analysis Centre, Wuhan University. Data collected on 15 August 2024, sampled every 30 s, were analyzed. On this day the constellation encompassed more than 30 satellites equipped with five clock classes: rubidium standards on GEO and IGSO platforms, rubidium and hydrogen masers on MEO spacecraft, and hydrogen masers on IGSO vehicles [16]. Eight satellites were purposely chosen to reflect diversity in orbit type, clock physics, system series and launch date: BDS-2 PRN 02, 04 (GEO-Rb), PRN 07 (IGSO-Rb); BDS-3 PRN 40 (IGSO-H), PRN 32, 37 (MEO-Rb), PRN 25, 43 (MEO-H) (Table 1).

Table 1: Selected satellite related information.

Satellite ID	Clock type	Launch date	Clock bias trend
PRN 02	GEO-Rb	25 October 2012	Positive values monotonically increasing
PRN 04	GEO-Rb	31 October 2010	Negative values monotonically decreasing
PRN 07	IGSO-Rb	17 December 2010	Negative values monotonically increasing
PRN 25	MEO-H	24 August 2018	Positive values monotonically increasing
PRN 32	MEO-Rb	19 September 2018	Negative values monotonically decreasing
PRN 37	MEO-Rb	18 November 2018	Negative values monotonically increasing
PRN 40	IGSO-H	5 November 2019	Negative values monotonically decreasing
PRN 43	MEO-H	23 November 2019	Positive values monotonically increasing

The high-resolution clock-offset profiles of these eight spacecrafts, plotted in Figure 2 for 15 August 2024, reveal a monotonic decrease for PRN04, PRN32 and PRN40.While the clock bias time series for satellites PRN02, PRN07, PRN25, PRN37 and PRN43 exhibit a monotonically increasing trend, demonstrating sufficient representativeness.

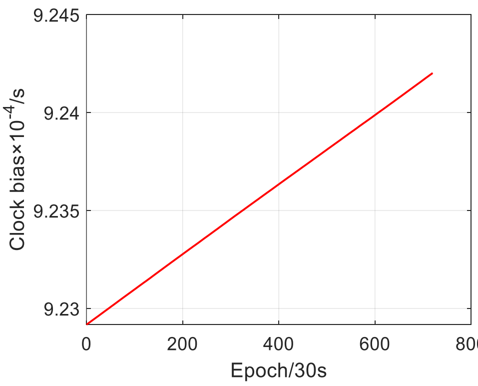

(a) PRN02

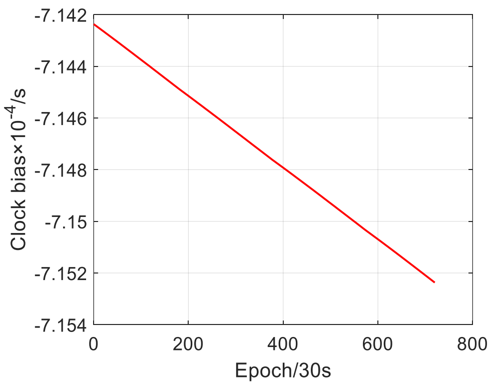

(b) PRN04

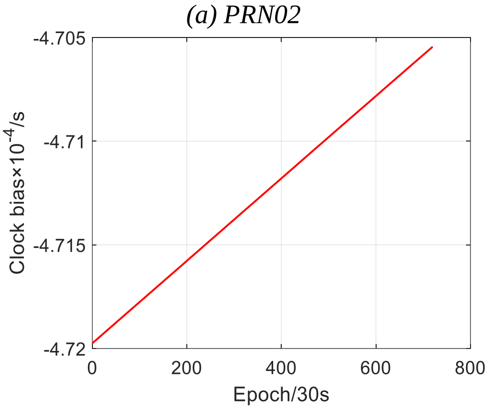

(c) PRN07

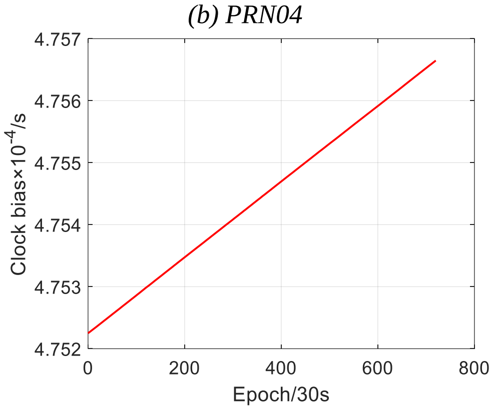

(d) PRN25

ISSN 2616-5775 Vol. 9, Issue 1: 94-102, DOI: 10.25236/AJCIS.2026.090112

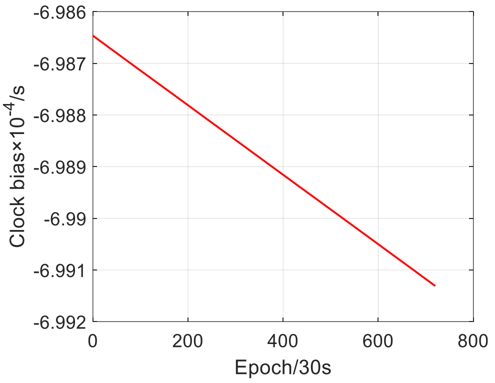

(e) PRN32

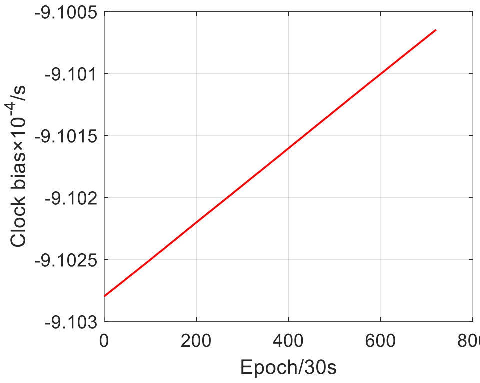

(f) PRN37

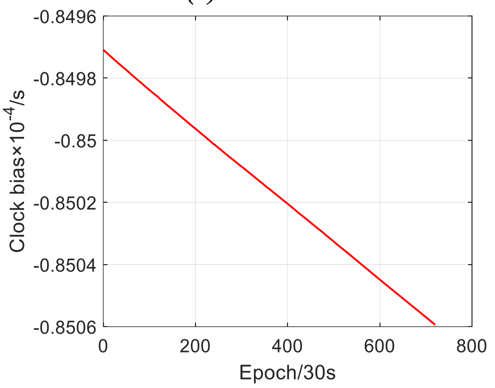

(g) PRN 40

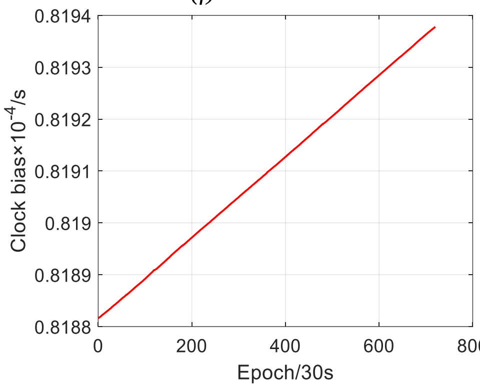

(h) PRN 43

Figure 2: Chart of clock bias variation for the PRN02, PRN04, PRN07, PRN25, PRN23, PRN37, PRN40 and PRN43 satellites.

3.2 Forecast results and analysis

To benchmark the developed predictor, 12 h of high-precision SCB estimates prior to 00:00–06:00 on 15 August 2024 were ingested to build a QPM, an LPM and a GM(1,1) model, whose outputs were then compared against the recorded biases for the subsequent 6 h. Forecast results were compared against precise SCB data for the same period released by Wuhan University GNSS Analysis Centre, calculating the forecast error for each model. The precision of the Wuhan University GNSS Analysis Centre SCB estimates permits their designation as the effective true values in the validation exercise. The forecast accuracy of the optimized GM (1,1) model was compared and evaluated by calculating the Root Mean Square (RMS) error. The RMS formula is as follows:

$$RMS = \sqrt{\frac{1}{n}\sum_{i=1}^{n}\left(y_i - \hat{y}_i\right)^2} \tag{23}$$

The variations in forecast errors and statistical results for each model are presented in Figure 3 and Table 2:

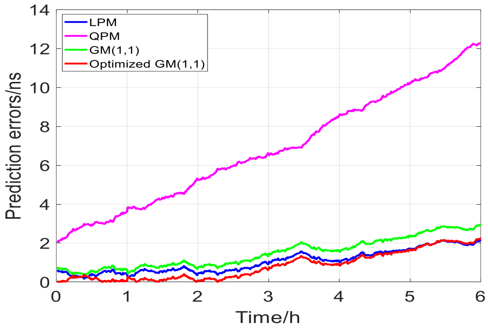

(a) PRN02

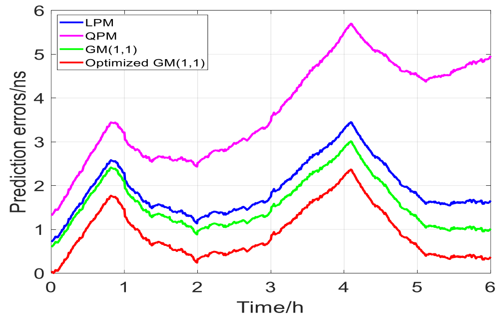

(b) PRN04

ISSN 2616-5775 Vol. 9, Issue 1: 94-102, DOI: 10.25236/AJCIS.2026.090112

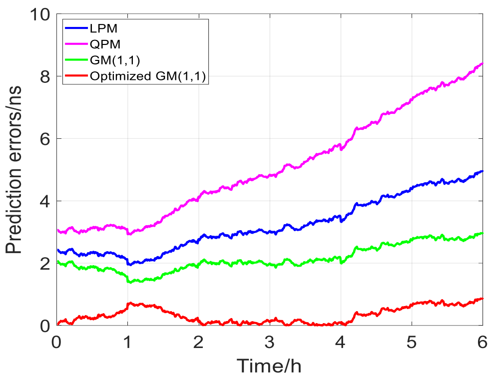

(c) PRN07

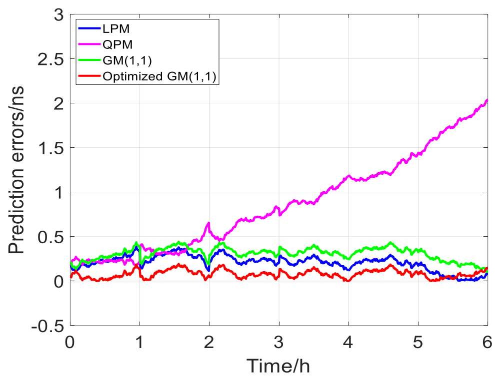

(d) PRN25

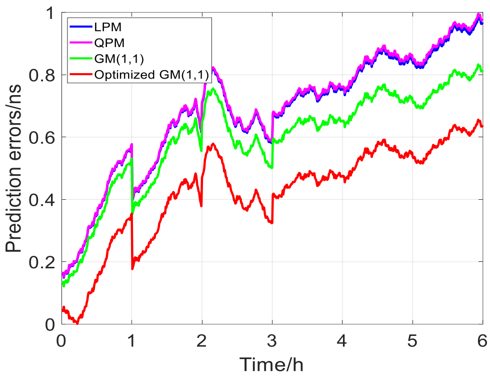

(e) PRN32

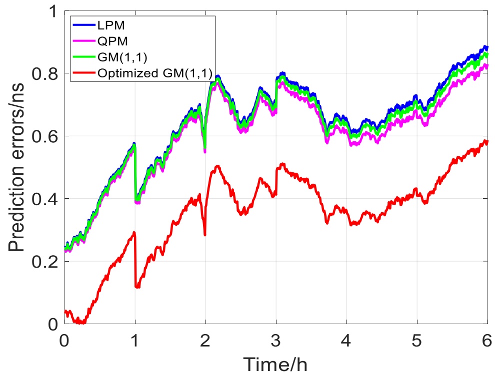

(f) PRN37

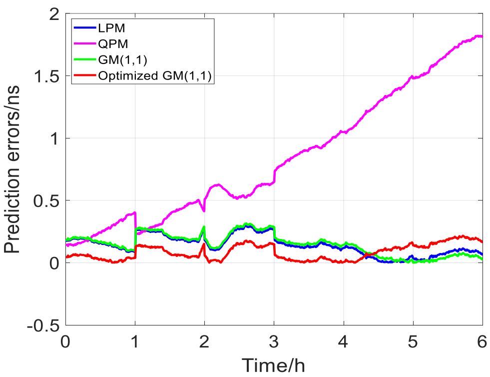

(e) PRN40

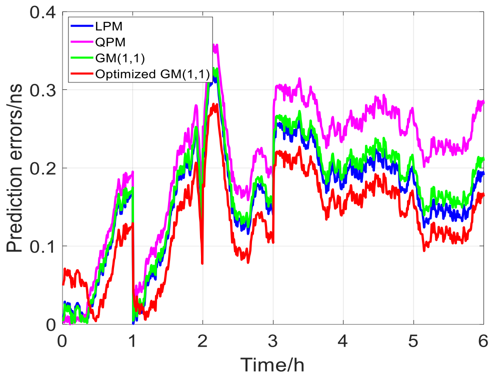

(f) PRN43

Figure 3: Forecast error variation chart of 6 h satellite clock bias

Table 2: Statistical results of satellite clock bias forecast error (unit: ns)

Model	PRN02	PRN04	PRN07	PRN25	PRN32	PRN37	PRN40	PRN43	Average
LPM	1.19	2.01	1.56	0.23	0.71	0.66	0.16	0.18	0.84
QPM	7.42	3.88	0.53	1.01	0.72	0.63	0.98	0.23	1.93
GM (1,1)	1.66	1.67	0.57	0.32	0.62	0.65	0.17	0.19	0.73
Optimized GM (1,1)	1.08	1.09	0.40	0.09	0.45	0.38	0.10	0.15	0.47

Analysis of Figure 2-3 and Table 2 reveals:

The forecast error of SCB data using the GM (1,1) model optimized with initial conditions shows a marked reduction compared to the other four models. The forecast error trajectory of the proposed GM (1,1) variant mirrors the standard version; however, the absolute errors are markedly compressed across the entire horizon. Furthermore, as the forecast lead time increases, the absolute values of forecast errors for the majority of satellites gradually rise. This indicates a substantial improvement in the forecasting accuracy of the initial condition-optimized GM (1,1) model. Furthermore, when employing the initial condition-optimized GM (1,1) model for SCB forecasting—using 12 h clock offset data to model future 6 h clock bias data—the forecast accuracies for the three BDS-2 satellites were 1.08

ns,1.09 ns and 0.40 ns, respectively, representing substantial improvements over the QPM, LPM and traditional GM (1,1) model. Comparative metrics reveal that the initial-condition refinement boosts predictive accuracy by 35.04 %, 34.75 % and 30.18 % in the evaluated instances. For the five satellites of BDS-3, the forecast accuracies were 0.09 ns, 0.45 ns, 0.38 ns,0.10 ns and 0.15 ns, respectively. Compared with the QPM, LPM and traditional GM (1,1) model, the forecast accuracy also showed a substantial improvement. Accuracy improvements attributable to the refined initial condition reached 35.04 %, 34.75 % and 30.18 % for the respective scenarios.

4. Conclusion

This study proposes a method for generating initial conditions using components from known SCB sequences, thereby improving the traditional GM (1,1) model. This approach fully utilizes known SCB data while specifically considering the impact of temporal sequencing on forecast outcomes. The convergence of analytical insight and experimental metrics demonstrates that optimizing the initial condition empowers the GM (1,1) model to satisfactorily reproduce future SCB values. Compared with QPM, LPM and the traditional GM (1,1) model, it exhibits a marked improvement in forecasting accuracy. Furthermore, the trend in forecast error variation for the initial condition-optimized GM (1,1) model aligns closely with that of the conventional GM (1,1) model. This indicates that the stability of the clock bias forecast achieved by the GM (1,1) model developed in this study remains fundamentally consistent with that of the traditional GM (1,1) model. In future research, targeted pre-processing based on the specific characteristics of SCB data could be employed to further enhance the forecasting accuracy and stability of the optimized GM (1,1) model.

Acknowledgements

This study is supported by the National Natural Science Foundation of China (No. 12403080), the China Postdoctoral Research Performance Evaluation and Assessment Funding Project (YJC20251197), the China Postdoctoral Science Foundation Funded Project (No.2024M764304), the Postdoctoral Fellowship Program of CPSF (No. GZC20233565) and the Natural Science Basic Research Program in Shaanxi Province of China (No.2023-JC-QN-0027).

References

[1] Wang J M, Li T, Xie D P, et al. Short-term forecasting of precise BeiDou satellite clock errors [J]. Science of Surveying and Mapping, 2020, 45(1): 33-41.

[2] Yu Y, Huang M, Duan T, et al. Satellite clock offset forecasting using a combination of particle swarm optimisation and weighted grey regression [J]. Journal of Harbin Institute of Technology, 2020, 52(10): 144-151.

[3] Li M, Huang T, Li W, et al. Precise point positioning with mixed single- and dual-frequency GNSS observations from Android smartphones considering code-carrier inconsistency[J]. Advances in Space Research,2024,74(6):2664-2679

[4] Yu Y, Huang M, Wang X Q, et al. Navigation satellite clock offset forecasting using grey models enhanced by least squares method[J]. Bulletin of Surveying and Mapping, 2019, (04):1-6.

[5] Mei, C S, Huang J H, Jiang K, et al. Application of a level-ratio discrete grey model in satellite clock error forecasting[J]. Journal of Wuhan University (Information Science Edition), 2021, 46(08): 1154-1160.

[6] Yi L, Xiong Y L, Xu L H. Comparison and accuracy analysis of two GPS satellite clock error forecasting models [J]. Surveying and Geoinformation, 2013, 38(02):17-19.

[7] Wang Y P, Lv Z P, Gong X C, et al. Analysis and comparison of forecast performance among several satellite clock error prediction models [J]. Geodesy and Geodynamics, 2015, 35(03): 373-378.

[8] Tan X R, Xu J N, He H Y, et al. Optimisation of initial conditions for the GM (1,1) model and its application in GNSS clock offset forecasting [J]. Geodesy and Geodynamics, 2022, 42(09): 919-924.

[9] Yu Y, Huang M, Wang C Y, et al. A new BDS-2 satellite clock bias prediction algorithm with an improved exponential smoothing method [J], Applied Sciences,2020,10(21):7456-7479.

[10] Wang Y H, Song X L, Gong J J. Application of error-corrected grey model in navigation satellite clock offset forecasting [J]. Journal of Time and Frequency, 2025, 48(01): 68-78.

[11] Cheng J H, Miao X Y, Zhao J Y, et al. A clock error forecasting method based on GM (1,1) and D-MECM [J]. Journal of Beijing University of Posts and Telecommunications, 2022, 45(02): 44-49.

ISSN 2616-5775 Vol. 9, Issue 1: 94-102, DOI: 10.25236/AJCIS.2026.090112

[12] Yang C W, Liu Z P, Xu Y M. Application of L-M algorithm-optimised grey model in GPS satellite clock offset forecasting [J]. Journal of Henan Polytechnic University (Natural Science Edition), 2020, 39(02): 47-52.
[13] Yu Y, Yang C P, Ding Y, et al. A hybrid short-term prediction model for BDS-3 satellite clock bias supporting real-time applications in data-denied environments[J]. Remote Sensing, 2025, 17(16):2888-2913.
[14] Song Q, Han C H. Robust grey model and its application in satellite clock error forecasting [J]. Journal of Surveying and Mapping Science and Technology, 2013, 30(05):471-474.
[15] Zhang Q H, Sui L F, Mou Z K, et al. Clock error forecasting algorithm using an improved grey model and its accuracy analysis [J]. Journal of Surveying and Mapping Science, 2012, 37(01): 51-53+114.
[16] Yu Y, Huang M, Duan T, et al. Enhancing satellite clock bias prediction accuracy in the case of jumps with an improved grey model[J]. Mathematical Problems in Engineering, vol 2020, Article ID 8186568, 11 pages, 2020.